Fracture 1977, Volume 1, ICF4, Waterloo, Canada, June 19 - 24, 1977

A CASE OF ELASTO-PLASTIC FLOW USING A NEW SPECIAL ELEMENT

J. L. Swedlow* and M. E. Karabin, Jr.*

ABSTRACT

Using a new special element for elasto-plastic flow, a nearly square, center-cracked plate of simulated A533 steel is analyzed. Selected results are examined locally to the crack's tip. It is found that a sharp transition in the distribution of deformation and stress occurs after the initial elastic response, and that this state is followed by fairly stable behavior over a considerable portion of the load range. Distribution of strain energy density is noted, and implications for use of the parameter J and for additional work are discussed briefly.

INTRODUCTION

Over the last several years, a variety of techniques has been devised for numerical analysis of strain and stress fields in elastic structures, and there have been several extensions of these techniques to account for non-linearities arising from material behavior and kinematic sources. Without reviewing the literature, we can simply observe that the confluence of the computer and these techniques has made a broad range of structural problems amenable to economical solution, largely on a routine basis.

Certain exceptions are to be noted; there are problems, typically involving singularities in the strain and stress fields, which are not well handled on the computer. Moreover, the degree to which solutions are regarded as satisfactory is dictated largely by the availability of analytic solutions which are used both in developing specialized numerical techniques and providing indices of their correctness. An important case is that of the sharp crack. Straightforward numerical analyses of such problems are generally evaluated in comparison to Williams's eigenanalysis of the local strain and stress fields [1], and one may only infer the singularities since the computer fails to replicate fully the nature of the local behavior. Using the Williams solution, special approaches have also been devised such that this theoretical response is merely scaled during the numerical procedure. Among such approaches is that of Gross and his co-workers [2] who employed collocation methods, special finite elements developed by Wilson [3] and Byskov [4] for example, and certain modified isoparametric elements as reported by Henshell and Shaw [5] and Barsoum [6], among others. All of these are of course formally limited to planar elasticity admitting only "small" or infinitesimal strains which, by association, suggests relatively low excitation levels.

For much higher excitation, Williams's solution is sometimes replaced by that reported independently by Hutchinson [7] and by Rice and Rosengren [8]. Finite element studies based on this "HRR model" were first reported by Hilton and Hutchinson [9] and indicate useful and interesting aspects

*Carnegie-Mellon University, Pittsburgh, Pennsylvania, USA.

of what may be termed fully plastic behavior with, again, the formal limitations of planar deformation and small strains.

These two analytical models have additional features in common. Both pertain only to fields local to the crack's tip, and each scales in terms of one parameter, respectively, K and J. Where Williams admits purely elastic response, however, the HRR model accounts only for plastic behavior; in a sense these models are then limit cases dual to one another. Missing is an analysis of the intermediate situation of combined response, or elasto-plastic flow. No work we have seen reported addresses the problem between the two limits which, inferentially, would correspond to high material toughness on the macroscale. By extension, the literature seems to have passed by the *process* whereby material in the immediate vicinity of a crack's tip goes from purely elastic through combined, or elasto-plastic response, to fully plastic behavior.

Certainly this issue has been contemplated in the context of numerical work, at least as long ago as the First Conference [10]. Missing then and still to be developed is an analytical base for subsequent computation so that, for example, the constraints Tracey [11] was obliged to meet are loosened. It may not be possible, however, to articulate the desired information analytically; for that reason, we have sought to determine the structure of crack-tip singularities numerically. The primary points of concern here thus become the radial and circumferential distribution of deformation and stress local to the crack's tip, and how closely to the crack's tip good data may be obtained. This paper contains certain parts of our first set of results, and we are able to see more clearly the transition. Moreover, we appear to have some characterization of the local fields rather close to the crack's tip for one arbitrarily selected situation. While a fuller picture must await scrutiny of additional solutions, we believe it useful to present the following information.

MODELING AND PROBLEM STATEMENT

The formulation is meant to be relatively simple so that we would obviate potential confusion between the numerics and the information being sought. It was envisaged that some sort of special element should be embedded in a field of constant strain elements, with which we have some operating experience, and that our first analyses would be for problems already solved by standard means. Thus the special element could eventually be evaluated on a comparative basis using a number of scales. With this objective in mind, we envisage the special element as a fan of sectors enclosing the crack tip (as in Figure 1a) connected to constant strain, or regular elements. For each sector, the increment in displacement components is easily written in terms of polar coordinates centered at the crack's tip (see Figure 1b). The cartesian components are

$$\delta u = \delta u_o + 2Ar\cos\theta + 2Cr\sin\theta + (E + F\theta)r^p\cos\theta - (G + H\theta)r^q\sin\theta$$
$$\delta v = \delta v_o + 2Br\sin\theta + 2Dr\cos\theta + (E + F\theta)r^p\sin\theta + (G + H\theta)r^q\cos\theta \qquad (1a)$$

and the corresponding cylindrical components are

$$\delta u_r = \delta u_o\cos\theta + \delta v_o\sin\theta + (A + B)r + (A - B)r\cos 2\theta + (C + D)r\sin 2\theta + (E + F\theta)r^p$$

$$\delta v_\theta = -\delta u_o\sin\theta + \delta v_o\cos\theta - (A - B)r\sin 2\theta - (C - D)r + (C + D)r\cos 2\theta + (G + H\theta)r^q \qquad (1b)$$

It is seen from (1) that $(\delta u_o, \delta v_o)$ are increments of a rigid translation vector; that $-(C - D)$ is a rigid rotation increment; that 2A, 2B, and (C + D) are increments of a uniform strain tensor over the sector, and that the special aspect of this element is reserved to the last terms of (1b). There, p and q are exponents to be determined, and E,F,G,H permit a modest amount of angular variation.

Straightforward if lengthy calculations give A,B,...,H in terms of node-point displacement increments, and one then finds the strain increments in terms of these quantities [12]. The stress increments relate to the strain increments in the usual form such that an energy-like functional Π may be computed. Requiring the first variation of this functional to vanish is tantamount to imposing equilibrium on the system [13]; we arrive at a set of conditions on the nodal displacement increments *and* the exponents p and q. The result is wholly within the general context outlined in [14].

Several aspects of this formulation are to be noted. To avoid intersector incompatibility, the exponent p and the exponent q are each common to all sectors of the special element. There will be, however, an incompatibility with the regular elements in which the special element is embedded; evaluation of this potential difficulty - for pure K_I and K_I plus uniform elastic strain excitation - shows the effect to be negligible. The same analyses show clearly that the simple, linear variation in the singular terms in (1b) represents the high circumferential gradients in stress and strain moderately well, provided enough sectors are used.* One must balance, therefore, a preference for many sectors against a corresponding growth in storage and CPU time requirements. The configuration in Figure 1a was used for detailed evaluation, and no restriction on the radial size of the special element was adduced in the preliminary analyses.

Apart from these matters, we note that the algebraic equations resulting from the formulation outlined above take the simultaneous form

$$K\delta u = \delta T \qquad (2)$$
$$\Pi = \text{minimum with respect to p and q} \rightarrow \Pi_e = \text{minimum}$$

where K is a stiffness matrix for the entire array of nodal displacement increments δu, δT is the corresponding vector of nodal force increments, and Π_e is the energy-like functional for the special element alone. In order to solve (2), we first solve for δu using standard algebraic methods; starting values for p and q are used in evaluating K. Next, Π_e is minimized with respect to the exponents, holding the special element's nodal displacement increments fixed. Then the stiffness equation is solved again using improved values of p and q, the process being iterated until the energy-like functional for the entire assembly of elements, regular and special, achieves a minimum (or as close to a minimum as we can discern from numerical analysis). This procedure is followed for each load step beyond the first, for which $p = q \equiv 1/2$, and appears to converge rapidly, typically

*A comparison formulation in the context of eight-noded isoparametric elements is being pursued by Marino [15]; fewer sectors appear to be needed and better representation of the angular behavior is expected.

in two cycles of iteration. Of course, the computation includes provision for accommodating local or global (elastic) unloading and other requirements for analysis of elasto-plastic flow described earlier [14]. This iterative scheme is necessary in spite of the simple formulation (1) because the problem, as posed, is highly non-linear with respect to the exponents. The formulation presents other operational difficulties in terms of data reduction, noted below, but we seem now to have found means for resolving them.

The next issue is to select a problem to solve by this method. After carefully considering a variety of alternatives, we have chosen the problem reported by Riccardella and Swedlow [16] for a first attempt. This problem, a center-cracked plate under uniform extension, was originally treated using constant strain elements alone, and the map was quite refined in the tip region of the crack (ℓ/a = 1/1024); 474 degrees of freedom were used in analyzing a quadrant of the plate. In the present analysis, the radius of the special element is designated as $2r_e$ and we have set $r_e/a = 1/128$; the surrounding mesh is less refined and the problem comprised only 348 degrees of freedom (plus the two exponents!). Within the special element, quadrature points are located at r/a ~ 0.0004, 0.002, 0.005, 0.008, 0.011, 0.014, and 0.015 so that the proximity of data points to the crack's tip in the two analyses is comparable. Having alternate solutions to the same problem has proven useful in developing confidence in the present results. While we have detected no spurious behavior, we had easy access to means for verifying this. Note, too, that the original solution [16] benefits from some experimental corroboration.

For completeness, it should be noted that the overall dimensions of the plate used in both studies, as described [16], are approximately 89 mm high × 76 mm wide, and the center crack is one-third the plate's width. The analysis is in plane strain. Loading was imposed via uniform extension Δ (as opposed to tension) of the two parallel edges farthest from the crack. The material is a representation of A533 grade B class 1 low alloy steel; actual tensile data were used in the computation, except for a smoothing operation to avoid the measured yield point instability. The specifics of the present analysis are thus the same as before except that we now use the special element and considerably fewer degrees of freedom.* We have adjusted the magnitude of the applied displacement increments to coincide with those in [16].

RESULTS AND DISCUSSION

A myriad of results presents itself, and we report here only those which provide the information outlined above. Thus we show data mainly for four load levels:

purely elastic (load step 1, Δ ≙ 0.0027 mm)

yield detected just beyond the special element (load step 38, Δ ≙ 0.017 mm)

yield extends through cross-section (load step 73, Δ ≙ 0.091 mm)

*CPU time per load step averaged just under 1.5 minute per increment on a Univac 1108 (Exec 2), considerably slower than an analysis using only regular elements. Much of the increase in CPU time is accounted for in the need to iterate, as described above.

average applied stress exceeds yield point (load step 93, Δ = 0.24 mm)

in which the yield point is taken from the smoothed stress-strain curve as 414 MPa (60 ksi in [16]).

It is usual in studies of this sort, to show certain standard types of information, e.g., the load-deflection curve, yield zones, etc. Since such information is neither different from that which has already been presented (e.g., [16,17]) nor especially pertinent to the present points of concern, we omit it here. Instead, we turn first to the angular variation of some quantitities. The node-point displacements at r/a ~ 0.008 (or r ~ 0.1 mm) appear in Figures 2a,b for θ = 0, 7.5, 15,...,180 deg. The horizontal displacement u is reduced by the crack tip motion u_o, and both it and the vertical displacement v are normalized on the (accumulated) applied extensional displacement Δ. Clearly, the data are smooth and they offer considerable detail in resolution of the angular behavior of the displacements.

Stress variation with angle is less satisfactory but not altogether objectionable. In Figures 3a,b we show the two in-plane principal stresses, normalized on the resultant applied load per unit area, or σ, as taken directly from the printed output. These data are also for r/a ~ 0.008 but pertain to the midline of each element, or to θ = 3.75, 11.25, 18.75,..., 176.25 deg. Note that the elastic results, for which gradients are highest, are smoothly described but, as yield becomes extensive, roughness develops in the data. Obviously, it would be straightforward to interpolate among these variations to describe the circumferential variation of stress.

We have confidence then in being able to establish the angular or circumferential variation in deformation and stress local to the crack's tip. Also examined, but not reported here, is the behavior of the data for smaller values of r/a. We observe a similar character of the data except for r/a ~ 0.0004 (or r ~ 0.005 mm) where the results become erratic. Data at this radial position are not shown in the sequel.

Radial variation may be depicted in two forms. We first show logarithmic plots of selected variables *vs* r/a, to provide a graphic sense of this behavior. In Figure 4a, $(u - u_o)/\Delta$ is plotted at θ = 90 deg; v/Δ at 0 → 180 deg appears in Figure 4b. In both, the elastic behavior is as expected although there is a clear influence of the relatively large transverse compressive stress known to be present in this problem.* Of more interest, perhaps, is the shift in slope of the data as excitation progresses. In the same vein, we show the behavior of $\sigma_1/\bar{\sigma}$ at θ → 0 deg in Figure 5, and strain energy density (arbitrarily normalized on $\bar{\sigma}\Delta/h$, where h ≙ 45 mm is half the specimen's height) at θ = 90 deg. In Figure 6 again, the original slopes are seen to be close to what is usually expected, being altered only by the transverse compressive stress (of magnitude $\bar{\sigma}$); the slopes then change as yield proceeds.

At this point, two characteristics of the results should be apparent. As yield proceeds from just beyond the special element to the nearest free surface (i.e., to general yield), there is a major change in the angular and radial distirubtions of displacements and stresses immediate to the crack's tip. This implies completion of a transitional process whose full

*While these graphic representations are useful, one's eye can misinterpret apparent slopes. Indeed, Barsoum takes advantage of this effect in an alternate formulation [18].

detail remains to be elucidated and reported. Second, the exponents p and q in (1) should provide a useful index to the transition. Thus, attention is turned to variation of exponents as the plate's boundaries are extended.

It is a simple matter to plot the exponents p and q through the range of extension considered here, and the result appears in Figure 7. Note the rapid drop from starting values of 0.5 and a recovery to about 0.3. It is also evident that p and q are not significantly different so that, although we have allowed for distinct values, future analyses might be expedited by equating the two exponents. The early part of the transition, i.e., $\Delta < 0.05$ mm, may be affected by the modeling process. Note that the exponents are minimal just as yield goes beyond the special element (step 38), and so the details of this phase of loading may be affected by the radial size of the special element. At gross yield (step 73), however, the yielded zone is very large with respect to the special element, and the behavior of p and q for $\Delta > 0.05$ mm is viewed as more realistic. Note further that p and q tend to rise gradually as yield continues beyond step 73; there seems to be some additional hardening of the material local to the crack's tip.

It is not, however, the quantities p and q that most interest us. Recalling from (1) that these exponents refer explicity to *increments* of displacement, we recognize that we need an integral of p and q *over the load path*. A look at a good table of integrals is sufficient to convince one that such quadrature is nontrivial, so that our next task is to establish exponents - if such exist - for accumulated displacements. That is, we would hope to find for any given value of the angle θ

$$u_r \sim \alpha_1 + \beta_1 r + \gamma_1 r^{p^*}$$

$$v_\theta \sim \alpha_2 + \beta_2 r + \gamma_2 r^{q^*} \qquad (3)$$

and then determine values of p* and q*. To this end we have examined data of the form shown in Figures 4a,b and numerically estimated these exponents. The procedure is based on fitting expressions of the form (3) to the data, assumes the α_i known from rigid motion as in (1b), and maximizes the coefficient of determination, typically to 0.99999, to obtain β_i, γ_i, and the exponents p*,q*. Averaging these values for several but not all sectors leads to the results tabulated:

step	p*	q*
1	0.4999	0.5002
38	0.3119	0.2463
73	0.2321	0.2404
93	0.2794	0.2982

Close examination of the numerical results of the fitting of (3) to the finite element data reveals the process to be quite stable, except perhaps for some variation at step 38. In order to establish behavior in this load range, therefore, we need to make further computations for different values of $2r_e$ (the radial size of the special element). For the present, however, we see from this and earlier analyses, e.g., [10,16,17], that behavior in the immediate vicinity of the crack's tip is described by three and possibly four stages: an essentially elastic response as described by Williams [1], a sharp transition, a relatively stable period, and a slow transition to another state possibly that described by the HRR model [7,8] or possibly something else.

The foregoing procedure may be repeated for strains owing to their direct relation to displacements. Hence one could write, for example,

$$\varepsilon_r \sim \beta_1 + p^* \gamma_1 r^{p^*-1} \qquad (4)$$

and carry through the necessary calculations. The same results as shown above would obtain. On the other hand, stresses are not so easily treated. There is no basis analogous to (4) upon which to draw because the stresses derive from integration (over the load path) of stress increments which, in turn, relate to the strain increments through the inverse flow rule. Indeed, Barsoum's expression in [18] suggests that many such formulae might work, provided that sufficient flexibility is available through the parameters used. We thus defer this type of reduction of the stress data, pending further study as suggested below. It is noted, however, that the stress data evince the succession of stages noted and in particular, the sharp transition during initial yield.

Strain energy density also lacks a formal basis for reducing its radial behavior to a simple formula. In addition, it reflects the sharp transition to a much lesser degree. The data in Figure 6, as well as the HRR model, imply that W might reasonably be expected to take the form

$$W \sim W_0 + W_1 r^{s^*} \qquad (5)$$

where $s^* \sim -1$. Fitting the data to (5) by maximizing the coefficient of determination was therefore tried, with limited success. Typical values of the coefficient were in excess of 0.999, but only in the mid-range of θ. The mean values obtained for 60 deg $\lesssim \theta \lesssim$ 120 deg were

step	s*
1	-0.979
38	-0.858
73	-0.975
93	-1.012

While these values of s* correspond somewhat to expectation, we note that the result for step 1 is marginal. The reason, of course, is that W carries an inverse square root term in the elastic case, for which no provision is made in (5). Hence alternate formulae should be examined.

Of more interest, however is the observation for steps 73 and 93 that spurious results are obtained for $\theta \to 180$ deg, as opposed to the mid-range of θ, suggesting that yield near the crack's flank is engendered not so much by the crack itself as by the particular geometry in which the crack is embedded. Ahead of the crack ($\theta \lesssim 45$ deg) s* drops significantly but not precipitously to small values, and one is led to infer development of an inactive zone insofar as continuation of elasto-plastic flow is concerned. We have yet to examine and reduce fully the data describing strain energy density, largely because a proper basis must be established in place of (5); no figure is thus shown. We do see some if not total consistency with the HRR model at this stage.

There remains, however, the implication that possibly $s^* = s^*(\theta)$ which is consistent with our formulation, given the nature of the flow rule. To the extent that we are able to establish such behavior and its necessary dependence on the material's stress-strain curve, there is some effect on the path dependence associated with the parameter J. In considering this matter

more broadly, it is well to keep in mind that certain, perhaps critical, features differentiate the present analysis from those used to develop the arguments in favor of J as a characterizing parameter. Our formulation proceeds from an assumed (radial) variation of the displacement increments and not of the accumulated stresses. There is thus the obvious distinction between use of incremental (flow) and total (deformation) theories of plasticity, as well as between finite element and essentially analytical solution methods. In this paper, we treat a particular steel; our technique accommodates fairly arbitrary stress-strain behavior whereas the HRR model is limited to a specific type of stress-plastic strain response. It is not yet known whether these factors affect the results and, if so, in what respect(s). Continuation of the work reported here is designed to provide further information both by use of alternate numerics [15] and by repeating this analysis with alternate material representations. We look forward to reporting additional findings soon.

CONCLUDING REMARKS

At the expense of much formulational detail, we have sought in this paper to provide an overview of a new approach for examining the structure of crack-tip behavior in an elasto-plastic material. Primary motivation is the need to follow the process whereby the canons of linear elastic fracture mechanics are transcended, and our model is constructed accordingly. This model, exemplified by (1), is intended to capture the essential feature of behavior local to the crack's tip by including in the displacement increments terms of r^p and r^q. At the same time, we have avoided any further presumption of the response, particularly that of the role of material which is properly left to the flow rule.

It is gratifying to observe in this first set of results that the procedure appears quite workable. In fact we are able to elicit deformation and stress behavior close to the crack's tip ($10^{-3} < r/a < 10^{-2}$), and to show reasonable detail of the circumferential distribution. In this connection it is well to recall that the angular gradients of, say, stress exceed the radial gradients to a remarkable degree [19], which any formulation for this sort of analysis must take into account.

Certain matters nonetheless require further attention. From the standpoint of numerics, it is clear that the formulation (1), while containing little presumption of eventual response, does not lend itself to simple data reduction procedures. Thus a direct comparison of our results to others in terms, for example, of exponents, is impeded. On the other hand, we are not aware of detailed, local, physical measurements which might be used to corroborate such parameters. It does seem, however, that the present availability of displacement data lends itself to such comparison for actual materials, and we would be interested in collaborating with other researchers who are able to develop the companion physical data.

It would be on this basis that other matters are ultimately resolved. We see, for example, some influence of overall goemetry even for very small values of r/a. While this may be an effect assignable to numerics, we think it may be real in the sense suggested by Larsson and Carlsson [20]. Of greater interest is the matter of material influence. As noted above, the differences between our approach and results and others - notably the HRR model - is thought to transcend analytical methodology and, as this is written, work is under way to carry the question further. We hope to achieve a basis for definitive resolution of such differences as may be

shown to exist so that the utility of this and other efforts may find a place in serving the more practical need of having fracture criteria for tough materials.

ACKNOWLEDGMENTS

This work was supported by the National Aeronautics and Space Administration through NASA Research Grant NGR 39-087-053.

REFERENCES

1. WILLIAMS, M. L., Journal of Applied Mechanics, 24, 1957, 109-114.
2. GROSS, B. E., SRAWLEY, J. W., and BROWN, W. F. Jr., NASA TN D-2395, 1964; GROSS, B. E. and SRAWLEY, J. E., NASA TN D-2603, 1965, NASA TN D-3092, 1965, and NASA TN D-3295, 1966.
3. WILSON, W. K., Stress Analysis and Growth of Cracks, Part 1, STP 513, American Society for Testing and Materials, Philadelphia, 1972, 90-105.
4. BYSKOV, E., International Journal of Fracture Mechanics, 6, 1970, 159-167.
5. HENSHELL, R. D. and SHAW, K. G., International Journal for Numerical Methods in Engineering, 9, 1975, 495-507.
6. BARSOUM, R. S., International Journal of Fracture, 10, 1974, 603-605.
7. HUTCHINSON, J. W., Journal of the Mechanics and Physics of Solids, 13, 1968, 13-31.
8. RICE, J. R. and ROSENGREN, G., Journal of the Mechanics and Physics of Solids, 13, 1968, 1-12.
9. HILTON, P. D. and HUTCHINSON, J. W., Engineering Fracture Mechanics, 3, 1971, 435-451.
10. SWEDLOW, J. L., WILLIAMS, M. L. and YANG, W. H., Proceedings of the First International Conference on Fracture, The Japanese Society for Strength and Fracture of Materials, Japan, 1966, 259-282. See also HOPKINSON, B., Transactions of the Institution of Naval Architects (London), 60, 1913, 232-234.
11. TRACEY, D. M., Ph.D. Dissertation, Brown University, 1973.
12. SWEDLOW, J. L., Report SM 74-10, Department of Mechanical Engineering, Carnegie-Mellon University, 1974.
13. JONES, D. P. and SWEDLOW, J. L., International Journal of Fracture, 11, 1975, 897-914.
14. SWEDLOW, J. L., Computers and Structures, 3, 1973, 879-898.
15. MARINO, C., unpublished work, 1976.
16. RICCARDELLA, P. C. and SWEDLOW, J. L., Fracture Analysis, STP 560, American Society for Testing and Materials, Philadelphia, 1974, 134-154.
17. SWEDLOW, J. L., International Journal of Fracture Mechanics, 5, 1969, 33-44.
18. BARSOUM, R. S., International Journal of Fracture, 12, 1976, 443-446.
19. CLAUSING, D. P., private communication, 1968.
20. LARSSON, S. G., and CARLSSON, A. J., Journal of the Mechanics and Physics of Solids, 18, 1973, 263-277.

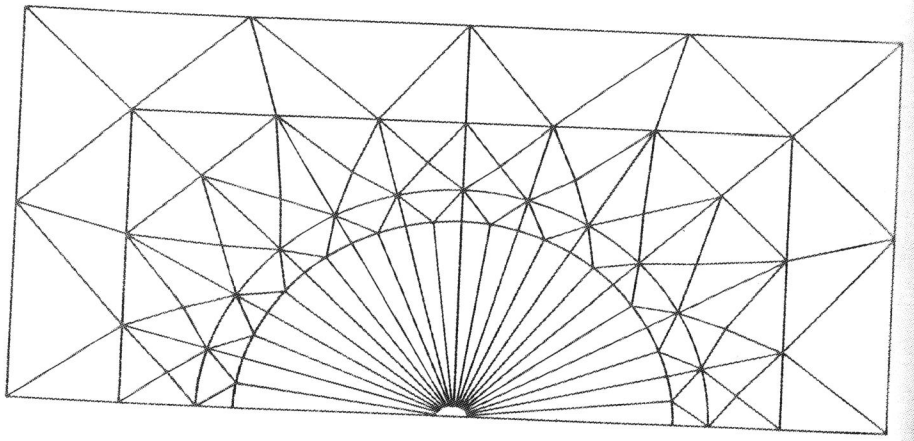

Figure 1a Array of sectors comprising special element, connected to regular elements

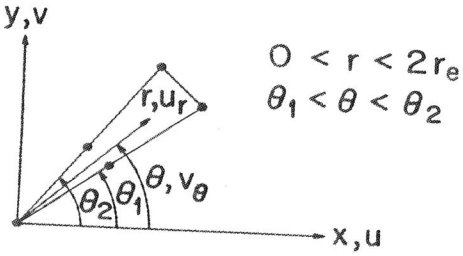

Figure 1b A typical sector of the Special element

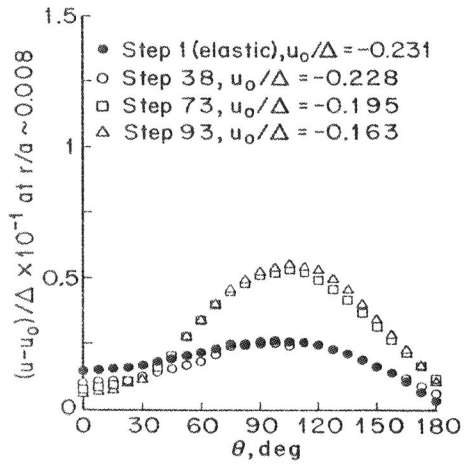

Figure 2a Angular variation of node-point displacements $(u-u_o)/\Delta$ at r/a ~ 0.008 for four load steps.

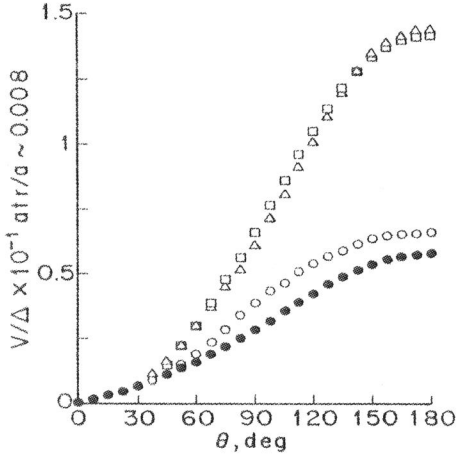

Figure 2b Angular variation of normalized node-point displacements v/Δ at r/a ~ 0.008 for four load steps.

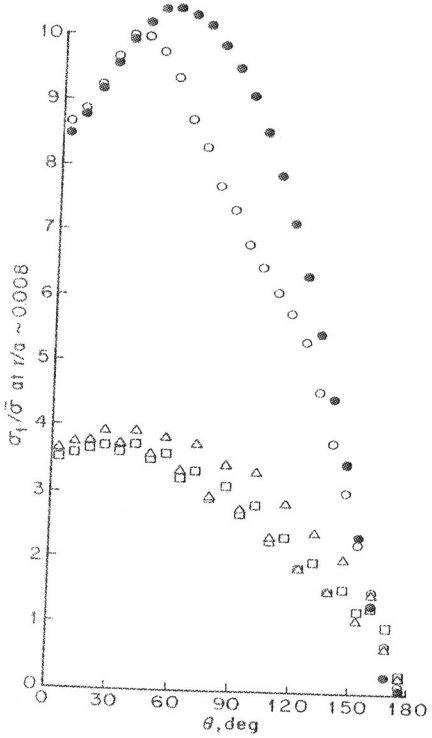

Figure 3a Angular variation of normalized larger in-plane principal stress $\sigma_1/\bar{\sigma}$ at r/a ~ 0.008 for four load steps (interior element values)

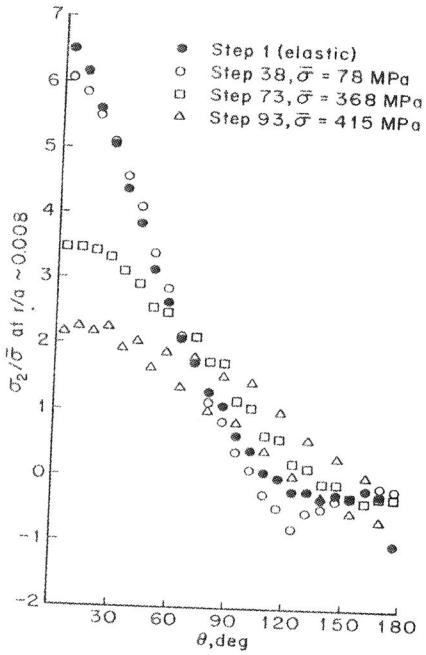

Figure 3b Angular variation of normalized smaller in-plane principal stress $\sigma_2/\bar{\sigma}$ at r/a ~ 0.008 for four load steps (interior element values)

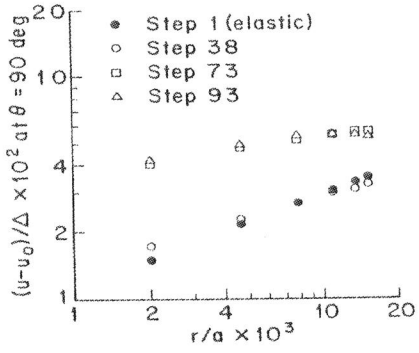

Figure 4a Radial variation of $(u-u_0)/\Delta$ at θ = 90 deg for four load steps

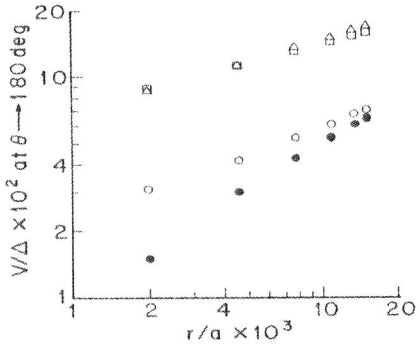

Figure 4b Radial variation of v/Δ at θ → 180 deg for four load steps

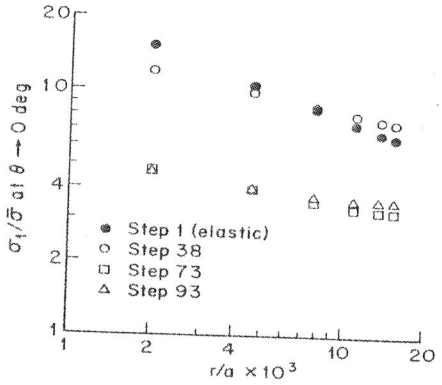

Figure 5 Radial variation of $\sigma_1/\bar{\sigma}$ at $\theta \to 0$ deg for four load steps

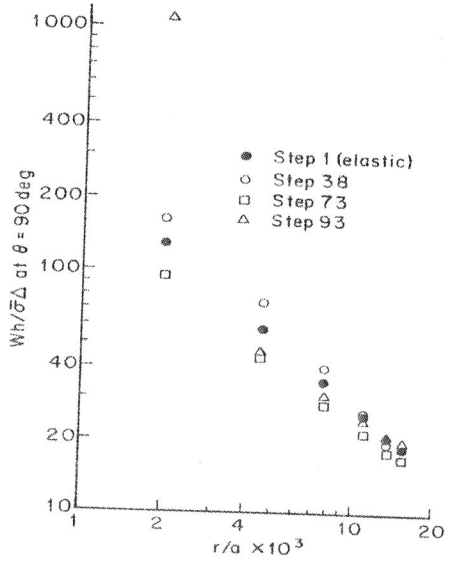

Figure 6 Radial variation of normalized strain energy density $Wh/\bar{\sigma}\Delta$ at $\theta = 90$ deg for four load steps

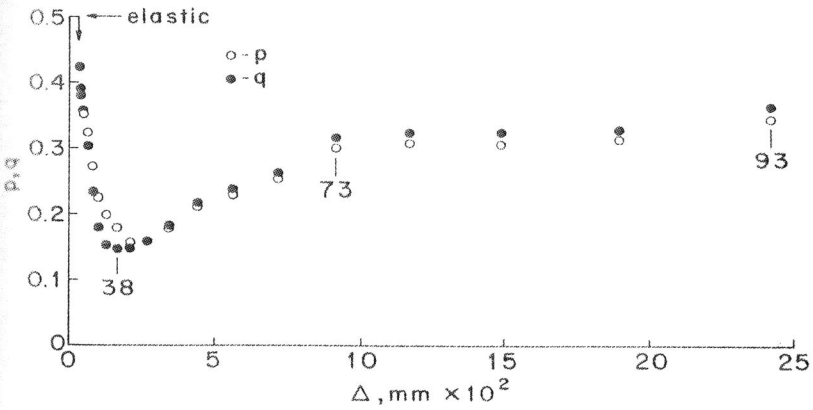

Figure 7 Exponents p and q in equation (1) as extension Δ progresses, for every fifth load step